In Vitro Cell.Dev.Biol.—Animal (2013) 49:638–652
DOI 10.1007/s11626-013-9628-y

Polarized neural stem cells derived from adult bone marrow stromal cells develop a rosette-like structure

Shahram Darabi · Taki Tiraihi · Atefeh Ruintan · Hojatt Allah Abbaszadeh · AliReza Delshad · Taher Taheri

Received: 30 November 2012 / Accepted: 26 April 2013 / Published online: 15 June 2013 / Editor: T. Okamoto

Abstract Bone marrow stromal cells (BMSCs) were reported to form floating aggregation of cells with expression of nestin, a marker for neural stem cells (NSCs). The purpose of this investigation is to evaluate the morphology and the molecular markers expressed by NSCs derived from these neurospheres. The BMSCs were isolated from Sprague Dawley rats and evaluated for osteogenesis, lipogenesis, and expression of fibronectin, CD90, CD106, CD31, and Oct4. The BMSCs were cultured with Dulbecco's modified Eagle's medium (DMEM)/F12 containing 15% fetal bovine serum, then with DMEM/F12 containing 2% B27, basic fibroblast growth factor, and epidermal growth factor. The cell aggregates or spheres were stained with acridine orange, which showed that the neurospheres comprised aggregated cells at either premitotic/postsynthetic (PS), postmitotic/presynthetic (PM) phases of cell cycle, or a mixture of both. The NSCs harvested from the neurospheres were polar with eccentric nucleus, and at either a PS or a PM cell cycle phases, some cells at the latter phase tended to form rosette-like structures. The cells were immunostained for molecular markers such as nestin, neurofilament 68 (NF68), NF160, and NF200 and glial fibrillary acidic protein (GFAP). Myelin basic protein (MBP), the pluripotency (Oct4, Nanog, and SOX2), and the differentiation genes (NeuroD1, Tubb4, and Musashi I) were also evaluated using reverse transcription polymerase chain reaction (RT-PCR). Nestin, NF68, NF160, NF200, GFAP, O4, and N-cadherin were expressed in the NSCs. The percentage of immunoreactive cells to nestin was significantly higher than that of the other neuronal markers. MBP was not expressed in BMSCs, neurospheres, and NSCs. The neurospheres were immunoreactive to GFAP. RT-PCR showed the expression of NeuroD1 and Musashi I. The pluripotency gene (SOX2) was expressed in NSCs. Oct4 and Nanog were expressed in BMSCs, while Oct4 and SOX2 were expressed in the neurosphere. This indicates that a pluripotency regularity network existed during the transdifferentiation of BMSCs into NSCs. Image processing of the neurospheres showed that the cells tended to form radial patterns. The conclusion of this study is that the NSCs generated from the BMSC-derived neurospheres have the morphology and the characteristics of neuroepithelial cells with tendency to forming rosette-like structures.

S. Darabi · T. Tiraihi · H. A. Abbaszadeh
Department of Anatomical Sciences, Faculty of Medical Sciences, Tarbiat Modares University, Tehran, Iran

S. Darabi
e-mail: shahram2005d@yahoo.com

H. A. Abbaszadeh
e-mail: hoomanabs@yahoo.com

T. Tiraihi · A. Ruintan · T. Taheri
Shefa Neurosciences Research Center, Khatam Al-Anbia Hospital, Tehran, Iran

A. Ruintan
e-mail: atefeh.ruintan@yahoo.com

T. Taheri
e-mail: khatam_sci@yahoo.com

A. Delshad
Department of Anatomy, Shahed University, Tehran, Iran
e-mail: delshada@yahoo.com

T. Tiraihi (✉)
Department of Anatomical Sciences, School of Medical Sciences, Tarbiat Modares University, P.O. Box 14155-4838, Tehran, Iran
e-mail: takialtr@modares.ac.ir

T. Tiraihi
e-mail: ttiraihi@gmail.com

Keywords Rosette-like · Neural stem cells · Neurospheres · BMSCs

Introduction

Cell therapy is considered an option for treating neurological disorders; for instance, neurological tests in the rat stroke model gave better results after intra-arterial injection of bone marrow stromal cells (BMSCs) (Li et al. 2001), and similar results were documented in other disorders. Lu et al. (2001) reported the benefit of administrating rat BMSCs in treating traumatic brain injury intravenously. Likewise, BMSCs therapy improved seizure in epileptic rats (Abdanipour et al. 2011b).

On the one hand, production of neuronal phenotype by in vitro induction of BMSCs was reported by Woodbury et al. (2000), who utilized β-mercaptoethanol (BME) with 20% fetal bovine serum (FBS) as preinducer and BME, dimethyl sulfoxide (DMSO), and butylated hydroxyanisole (BHA) as inducers, while Hung et al. (2002) combined BME and retinoic acid for the induction. Alternatively, growth factors such as epidermal growth factor (EGF) and brain-derived neurotrophic factor for inducing the BMSCs into neural phenotype were applied by Sanchez-Ramos et al. (2000); besides, simple metabolic substances (isobutylmethylxanthine and dibutyryl cAMP as inducers) and 5-azacytidine, a demethylation agent, were used by Deng et al. (2001) and Kohyama et al. (2001), respectively. Other investigators employed different combinations of the above agents (Levy et al. 2003; Croft and Przyborski 2004; Hellmann et al. 2006), whereas coculturing BMSCs with fetal-derived neural cells resulted in their transdifferentiation into neuronal phenotype (Dezawa et al. 2004). While induction with simple compounds (BME, DMSO, and BHA) was described by Woodbury et al. (2000), Lu et al. (2004) considered the transdifferentiation by these chemicals as an artifact rather than actual induction mechanism; a similar view was adopted by Neuhuber et al. (2004), who suggested that this mode of transdifferentiation was not optimal for induction. Croft and Przyborski (2004) disclosed that the expression of neural markers was not consistent with typical development; thus, shedding doubts on the transdifferentiation process; however, Suon et al. (2004) considered that BMSCs transdifferentiation could occur only transiently. Recently, Barnabé et al. (2009) reported that the transdifferentiated cells could have neural markers but they were not functional.

Meanwhile, many of the above chemicals used in the transdifferentiation were mutagenic, carcinogenic, or teratogenic agents (Ghorbanian et al. 2010). Also, the yield of the transdifferentiated cells was confirmed to be low; for example, Woodbury et al. (2000) documented that the maximum yield was 51%, while Deng et al. (2001) mentioned 13%; it may be caused by high cell death associated with the transdifferentiation utilizing BME, DMSO, and BHA (Barnabé et al. 2009). Furthermore, Chen et al. (2006) suggested that exploring better methods for in vitro differentiation with better characterization of the transdifferentiated cells was essential. One of the approaches was to derive neural phenotypes by producing neurospheres from bone marrow stromal cells; the generated cells had the properties of neural progenitor cells (Hermann et al. 2004). In this study, cellular and molecular evaluations of primitive neural stem cells obtained from BMSCs-derived neurosphere have been investigated, where they generated clusters similar to rosette-like structures.

Materials and Methods

Cell preparation. The use of the animals in this study was approved by the Ethical Committee at Tarbiat Modares University (Tehran, Iran) in accordance to Helsinki Ethical code about laboratory animal use. The bone marrow cells were collected aseptically from the femurs of adult female Sprague Dawley rats weighing 200–250 g, which were anesthetized with ketamine and xylazine (50/kg and 10 mg/kg, respectively). A drill hole (2×3 mm) was made in the proximal part of the femur, and the bone marrow was aspirated using a 21-gauge needle. The cells were washed three times with sterile phosphate-buffered saline (PBS), filtered through a 70-μm nylon filter mesh (BD Falcon, Heidelberg, Germany), cultured in Dulbecco's modified Eagle's medium/F12 (DMEM/F12; GIBCO-BRL, Eggenstein, Germany) containing 100 U/ml penicillin/streptomycin (GIBCO-BRL) and 10% heat-inactivated FBS (GIBCO-BRL), and were incubated at 37°C, 5% CO_2, and 95% relative humidity (RH) for 3 d. The non-adherent cells were discarded and the medium was replaced. When the cultures almost reached confluency, the adherent cells were harvested using 0.05% Trypsin–EDTA (Invitrogen, Paisley, Scotland), and they were subcultured at 1×10^4 cells/ml, resuspended in 20 ml medium, and replated onto 75 cm^2.

Mesodermal differentiation. The adipogenic differentiation was done according to Abdanipour et al. (2011a), and the BMSCs were induced by incubation at the third passage with adipogenic production medium containing 50 μg/ml indomethacin, 50 μg/ml ascorbic acid, and 100 nM dexamethasone (Sigma-Aldrich, Steinheim, Germany). After 3 wk, the lipid vacuoles were stained with Oil Red O (Sigma-Aldrich). Also, the osteogenic induction was done

according to Abdanipour et al. (2011a), and the BMSCs at the third passage were seeded for 21 d in osteogenic medium containing 10 mM β-glycerophosphate, 60 μM ascorbic acid, and 0.1 μM dexamethasone (Sigma-Aldrich). The calcium deposits and the osteogenic differentiation were identified by Alizarin Red S staining (Sigma-Aldrich).

Induction of BMSCs into floating spheres. For inducing the neurosphere-like structures, the BMSCs at the third passage were detached by incubation with 0.05% Trypsin/EDTA and cultured according to a protocol described by Reynolds and Weiss (1992) with some slight modifications. Briefly, the cell aliquots were plated (10^4 cells/cm^2) into six wells in neurosphere production medium consisting of DMEM/F12 supplemented with 20 ng/ml of EGF (Sigma-Aldrich), 20 ng/ml of basic fibroblast growth factor (bFGF; Chemicon, Hofheim, Germany) and 2% B27 (Invitrogen). The cell suspension was incubated for 1 wk at 37°C, 5% CO_2, and 95% RH.

Production of neural stem cells from neurospheres. The floating neurospheres were collected by centrifuging at 1,500 rpm for 5 min, and they were dissociated mechanically and enzymatically to single cells and suspended in DMEM/F12 supplemented with 2% B27 (Invitrogen) for 1 wk in 6-well plates containing poly-*l*-lysine (Sigma-Aldrich) coated cover slips. Immunohistochemical evaluation was done for CD90, CD106, CD31, nestin, NF68, NF200, and glial fibrillary acidic protein (GFAP) on the same cultured slices.

Rosette-like structure formation. The neurospheres were transferred to an adherent flask containing DMEM/F12 supplemented with 2% B27 (Invitrogen) and 5% FBS (GIBCO-BRL). Immunocytochemical evaluation was done

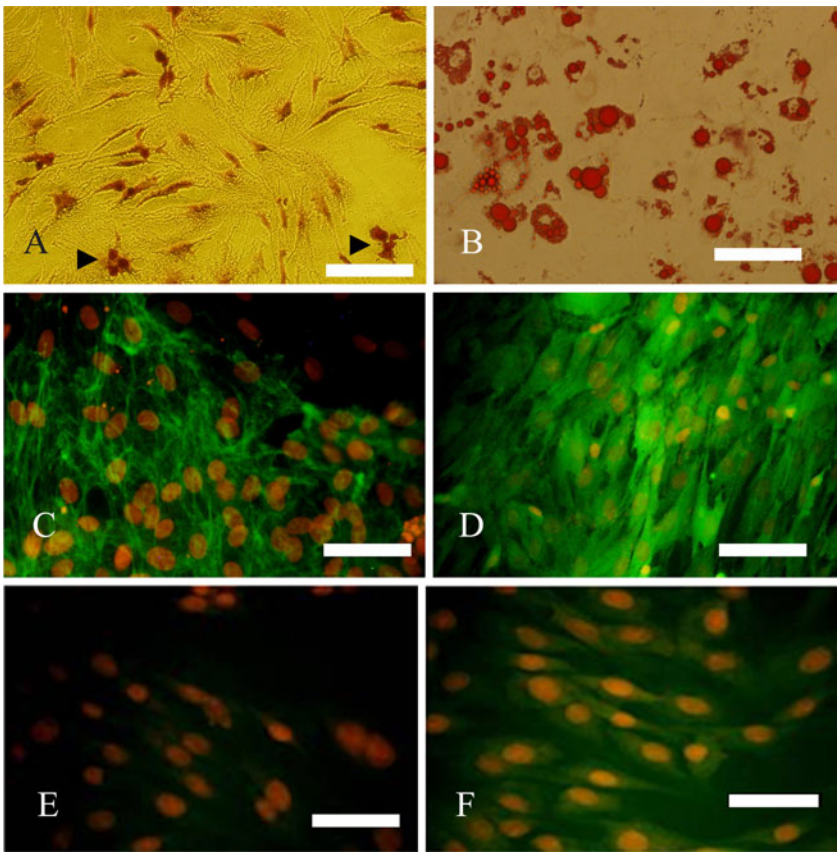

Figure 1. The bone marrow stromal cells (BMSCs) differentiated into osteogenic phenotype with formation of ossicle (*arrowhead*) stained with Alizarin Red S (*A*). *B*, The lipogenic differentiation of the BMSCs where several cells have multilocular lipid materials stained with Oil red stain. *C*, BMSCs immunostained with anti-fibronectin antibody (primary antibody), then incubated with secondary antibody conjugated with FITC, and counterstained with ethidium bromide. *D,* BMSCs immunostained with anti-CD90 antibody (primary antibody), then incubated with secondary antibody conjugated with FITC, and counterstained with ethidium bromide (a mesenchymal stem cell marker). *E*, BMSCs immunostained with anti-CD31 antibody (primary antibody), then incubated with secondary antibody conjugated with FITC, and counterstained with ethidium bromide (a specific marker for endothelial cell). *F*, BMSCs immunostained with anti-CD106 antibody (primary antibody), then incubated with secondary antibody conjugated with FITC, and counterstained with ethidium bromide (a mesenchymal stem cell marker) (*scale bar*: *A*, *B*=200 μm; *C*, *D*, *E*, *F*= 75μm).

for CD90, CD106, CD31, nestin, NF68, NF200, and GFAP on the same cultured slices.

Immunocytochemistry. The cells were fixed for 20 min at room temperature in 4% paraformaldehyde in 0.1 M phosphate buffer solution (pH 7.4). After washing twice in PBS, the cells were incubated for 20 min at room temperature (RT) in a blocking solution (2% goat serum, 5% FBS, with or without 0.3% Triton X-100 in 0.1 M phosphate buffer; Triton X-100 was used for cytoplasmic markers only). After an overnight incubation with the following primary antibodies: mouse anti-CD106 monoclonal antibody (1:300; Chemicon), mouse anti-CD31 monoclonal antibody (1:200; Chemicon), mouse anti-CD90 monoclonal antibody (1:300; Chemicon), rabbit anti-Oct4 polyclonal antibody (1:250; Bioss Inc., Woburn, MA), mouse anti-nestin monoclonal antibody (1:100; Chemicon), mouse anti-NF68 monoclonal antibody (1:200; Chemicon), mouse anti-NF160 monoclonal antibody (1:300; Chemicon), mouse anti-NF200 monoclonal antibody (1:400; Chemicon), mouse anti-N cadherin monoclonal antibody (1:200; Abcam, Cambridge, UK), mouse anti-GFAP monoclonal antibody (1:800; Sigma-Aldrich), mouse anti-O4 monoclonal antibody (1:300; Chemicon), mouse anti-Neu N monoclonal antibody (1:1,000; Abcam), and rabbit anti-c-Myc monoclonal antibody (1:300; Abcam), they were incubated for 2 h (RT) with relevant anti-mouse IgG FITC-conjugated (secondary antibody 1:100; Chemicon), anti-mouse IgG Alexa Fluor-conjugated (secondary antibody 1:500; Abcam), anti-rabbit IgG FITC-conjugated (secondary 1:1,000; Abcam), or anti-rabbit IgG Alexa Fluor-conjugated (secondary 1:500; Abcam) antibodies, washed twice in PBS, counterstained with ethidium bromide

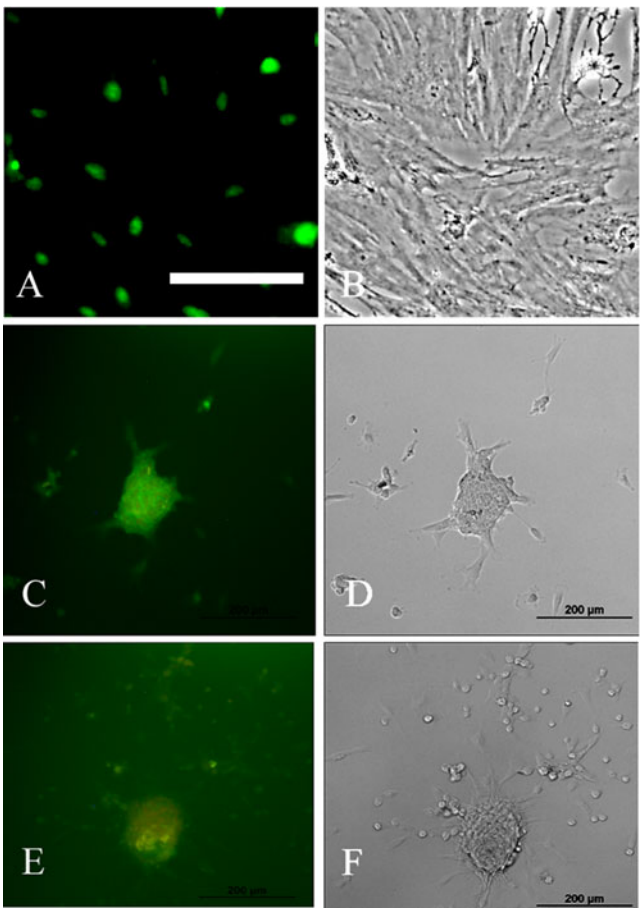

Figure 2. The immunostaining of the bone marrow stromal cells (BMSCs) and neurospheres (NS). *A*, Immunostaining of the NSCs anti-Oct4 (primary antibody); it was incubated with secondary antibody. *B*, A phase contrast image of *A*. *C*, Immunostaining of the NS with anti-nestin (primary antibody); it was incubated with secondary antibody and counterstained with ethidium bromide. *D*, A phase contrast image of *B*. *E*, The immunostaining of the NS glial fibrillary acid protein (primary antibody) followed by incubation with secondary antibody conjugated with FITC and counterstained with ethidium bromide. *F*, A phase contrast image of *E* (*scale bar*: *A*, *B*=100; *C*–*F*=200 μm).

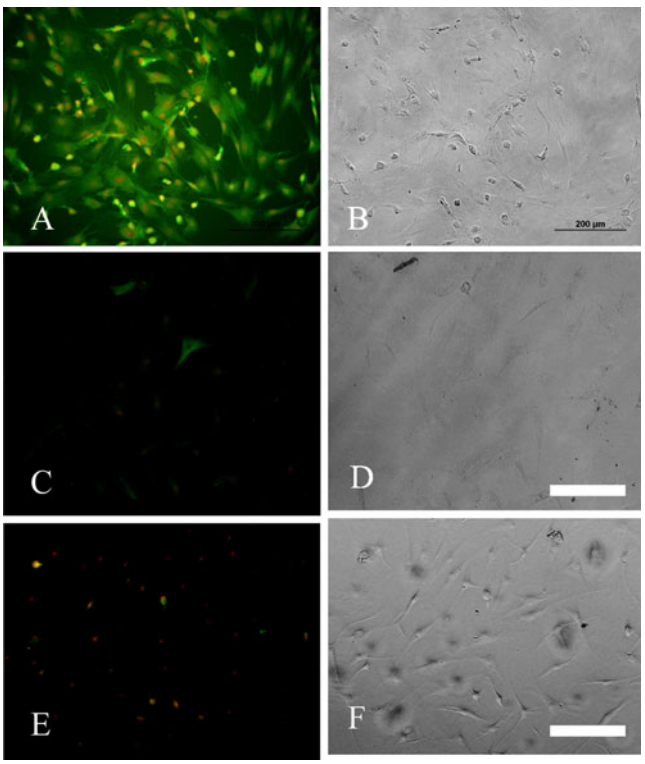

Figure 3. The immunostaining of the neural stem cells (NSCs) in adherent culture. *A*, Immunostaining of the NSC anti-nestin (primary antibody); it was incubated with secondary antibody and counterstained with ethidium bromide. *B*, A phase contrast image of *A*. *C*, Immunostaining of the NSCs with anti-glial fibrillary acidic protein (primary antibody); it was incubated with secondary antibody and counterstained with ethidium bromide. *D*, A phase contrast image of *B*. *E*, The immunostaining of the NSCs with anti-O4 (primary antibody) followed by incubation with secondary antibody conjugated with FITC and counterstained with ethidium bromide. *F*, A phase contrast image of *E* (*scale bar*=200 μm).

(10 μg/ml), and were visualized under a fluorescent microscope (Olympus 1x71, Olympus, Tokyo, Japan). The percentage of immunoreactive cells was estimated by counting 200 cells in five random fields (using the random number table).

Viability and neurospheres diameter. The viability test was determined by trypan blue exclusion assay. The mean neurosphere diameters at 1, 3, and 6 d of culturing were also measured on five randomly selected images. The neurospheres with more than 20 cells were considered in the study (Ge et al. 2010).

Acridine orange staining. The neurospheres and the suspended NSCs were seeded in a six-well plate and incubated at 37°C in 5% CO_2 for 24 h with 10 μg/ml of acridine orange (Merck, Darmstadt, Germany) dissolved in the incubation medium in PBS. After incubation, the neurospheres and the NSCs were harvested, suspended, washed with PBS, and recentrifuged at 1,000 rpm for 5 min. The supernatant was removed, and the pellet was resuspended in the incubation medium and 10 μl of the cell suspension was pipetted on a slide before putting them on a glass slide; within 30 min, the slide was analyzed using a fluorescent microscope (Olympus 1x71, Olympus). The viable and the dead cells were counted in a population of 200 cells (Rao et al. 2012; Vadivelu et al. 2012).

Neurospheres were stained with acridine orange and immunostained for N-cadherin, GFAP, and Neu N. The images were processed using Image J software (NIH, Bethesda, MD), and the edge of the cells was detected using edge find command. In another study, neurospheres were stained with acridine orange followed by ethidium bromide. The images were processed using Image J software (NIH). The colors of the images were split into blue, green, and red colors using split channels command, while the edge of the cells was detected using edge find command.

RT-PCR. The total cellular RNA was extracted from the BMSCs, the neurospheres, and NSCs using a high pure RNA isolation kit (Roche Biochemicals, Mannheim, Germany); it was followed by treatment with a DNase I (amplification grade kit; Invitrogen) and cDNA synthesis kit (MBI Fermentas, Vilnius, Lithuania). Reverse transcription polymerase chain reaction (RT-PCR) reactions and all of the procedures were performed in accordance to the instruction of the kits. The RT-PCR was performed with the following primers: fibronectin (gene accession number: NM019143, forward primer: CTGTCCTGTGGCTGTGTCC, backward primer: CAGTAGTAAAGTGTTGGCATGT, and product 221 bp), Oct4 (gene accession number: NM001009178, foreword primer: GGCTGTGTCCTTTCCTCT, backward

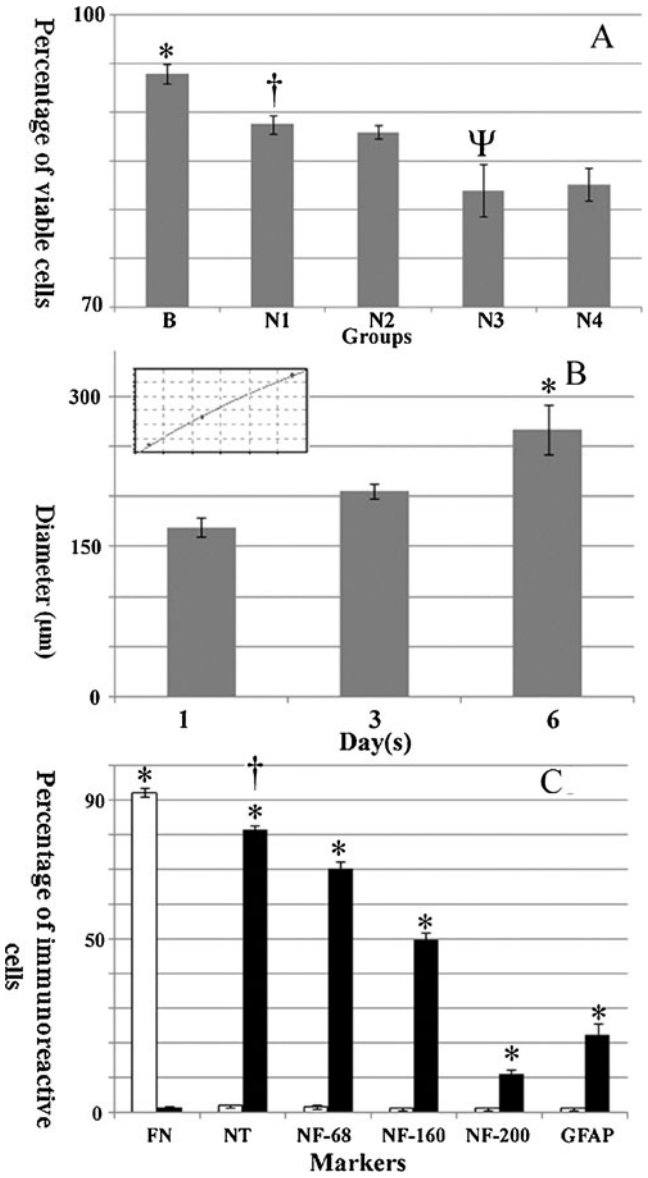

Figure 4. Histograms of the viability test, neurosphere diameter, and the percentage of the immunoreactive cells to different markers of bone marrow stromal cells (BMSCs) and neural stem cells (NSCs). *A*, A histogram of the percentage of the viable cells in the BMSCs (*B*) and NSCs (N) at days 1, 2, 3, and 4 (mean±SEM: N1, N2, N3, and N4, respectively). *Asterisk* is significantly higher than the other groups ($P<0.05$). *Dagger* is significantly higher than the other groups except N2 ($P<0.05$). *Greek small letter psi* is not significantly different from N4. *B*, A histogram of the diameter (mean±SEM) of the neurospheres at days 1, 3, and 6. *Inset* represents the nonlinear curve fitting of the neurosphere diameters against time (days); the growth pattern of the diameter shows logarithmic increase ($y=-55.4+(11\times\ln x)$, the standard error=0.1, and the correlation coefficient=0.99). *C*, A histogram of the percentage of the immunoreactive BMSCs (*solid white column*) and NSCs (*solid black column*) to fibronectin (*FN*), nestin (*NT*), neurofilament 68 (*NF68*), neurofilament 160 (*NF160*), neurofilament 200 (*NF200*), and the glial fibrillary acidic protein (*GFAP*) (all: mean± SEM). *Asterisk* is significantly higher than the other cell types ($P<0.05$). *Dagger* nestin is significantly higher than its value the in neural markers.

primer: TCTCTTTGTCTACCTCCCTTC, and product 217 bp), nestin (gene accession number: NM012987, foreword primer: AAGGCTCAGGAGTTCCAGG, backward primer: TACGGCTTTATTCAGGGAG, and product 244 bp), Nanog (gene accession number: NM001100781, foreword primer: TTCAAGACCAGCCTGTACT, backward primer: GCACTGGTTTATCATGGTAC, and product 219 bp), Tubb4 (gene accession number: NM080882, foreword primer: ACACACACACTCCACCTCC, backward primer: AACACACAGGGACCTATGG, and product 231 bp), Musashi I (gene accession number: NM148890, foreword primer: CACTGCTTATGGTCCGATGG,

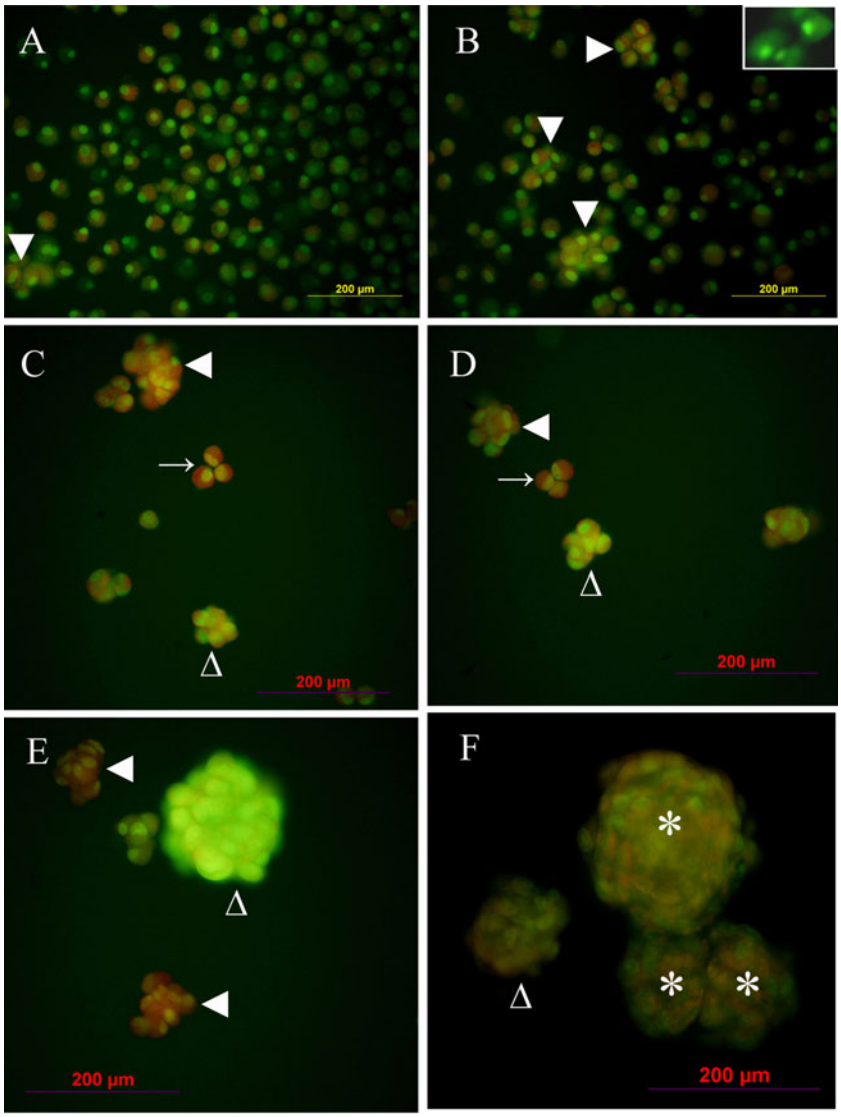

Figure 5. The acridine orange (AO) staining of the neural stem cells (NSCs) and the neurospheres (NS). *A*, The harvested NSCs stained with AO at the first hour, where the NSCs either *red* (at the postmitotic/presynthetic phase of the cell cycle, PM) or *green* (at the premitotic–postsynthetic phase of the cell cycle, PS); the nuclei have *green color* in both phases of the cell cycle. Most of the NSCs are polar; *arrowhead* represents the clustering of the NSCs into small groups of the same phase (PM). *B*, The harvested NSCs stained with AO at the fourth hour; the NSCs are either *red* (PM) or *green* (PS); the nuclei have *green color* in both phases of the cell cycle; *inset* shows higher resolution of the polar cells with eccentric nuclei. Most of the NSCs are polar; *arrowhead* represents the clustering of the NSCs into small groups of the same phase (PM). *C*, *D* The harvested NSCs stained with AO at day 1; the NSCs are either *red* (PM) or *green* (PS); the nuclei have *green color* in both phases of the cell cycle. Most of the NSCs are polar; *solid arrowhead* represents clustering of the NSCs into small groups of the same phase (PM). *Arrow* represents the clustering of the three NSC groups forming primitive rosette-like structure. *Empty arrowhead* represents the clustering of the NSCs into small groups of mixed phases (PM and PS). *E*, *F*, The harvested NSCs stained with AO at day 4, where the NSCs are either *red* (PM) or *green* (PS); the nuclei have *green color* in both phases of the cell cycle. Most of the NSCs are polar; *solid arrowhead* represents the clustering of the NSCs into small groups of the same phase (PM). *Empty arrowhead* represents the clustering of the NSCs into small groups of mixed phases (both PM and PS). *Asterisks* represent fusing neurospheres.

backward primer: GGTGAAGGCTGTCGCAATC, and product 274 bp), GFAP (gene accession number: NM017009, foreword primer: TAAGCGTCCATCCTGTTTG, backward primer: GGTTAGCAGAGGTGACAAGG, and product 226 bp), myelin basic protein (MBP; gene accession number: NM001025294, foreword primer: TTCCAAAG AGACCCACACTG, backward primer: AAGGTCG GTCGTTCAGTCAC (reverse; 247 bp)), NeuroD1 (gene accession number: NM019218, foreword primer: CTACTTGTTACCTTTCCCATGC, backward primer: GCTAAGGCAACGCAATAAC, and product 216 bp), SOX2 (gene accession number: NM001109181, foreword primer: CCGTTACAGACAAGGAAGG, backward primer: CAACGATATCAACCTGCATG, and product 194 bp), and the endogenous control (housekeeping) gene glyceraldehyde 3-phosphate dehydrogenase (foreword primer: CAAGGTCATCCATGACAACTTTG, backward primer: GTCCACCACCCTGTTGCTGTAG, and product 496 bp).

Statistical analysis. All the data in this study were compared by ANOVA, and the comparison among the groups means was performed by using ad hoc Tukey's test.

Results

The isolated BMSCs had typical morphology, differentiation (osteogenic and lipogenic), and markers including fibronectin (a marker for BMSCs), CD31 (a specific marker for endothelial cells), CD90, and CD106 (both mesenchymal stem cell markers). The cells were immunoreactive to fibronectin, CD90, and CD106 (see Fig. 1), while the BMSCs were immunoreactive to Oct4 (Fig. 2*A*). The neurospheres were immunoreactive to nestin, and only few cells were positive to anti-GFAP antibody (Fig. 2*C*, *E*, respectively). Figure 3 shows the immunostaining of NSCs with NF68, GFAP, and O4. The BMSC viability was significantly higher than the cultured NSCs at days 1, 2, 3, and 4 (Fig. 4*A*), while the viability of NSCs at day 1 was significantly higher than that at the fourth day (Fig. 4*A*) ($P<0.05$). The size of the neurospheres increased during culturing (days 1, 3, and 6) which was logarithmic in nature (Fig. 4*B*). The BMSCs showed high level of fibronectin expression, while the level of expression was trivial in the NSCs. The percentages of the NSCs expressing nestin, NF68, NF160, NF200, and GFAP were estimated. Nestin expression in the NSCs was

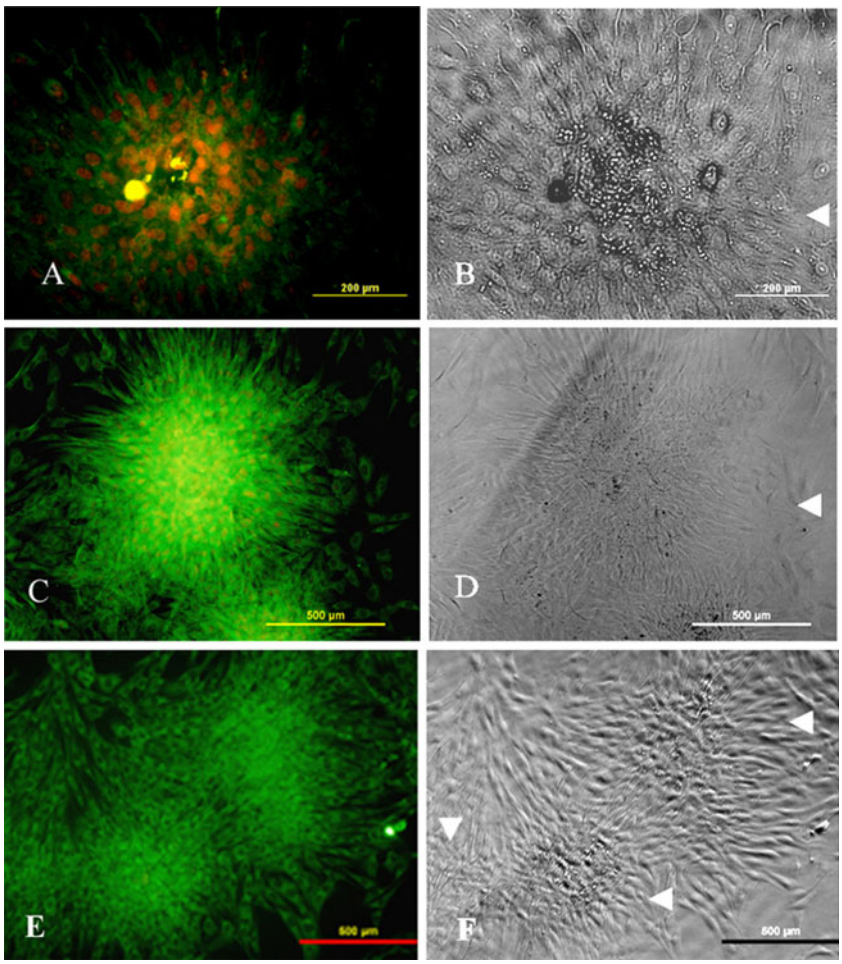

Figure 6. The immunostaining of the rosette-like structures in adherent culture. *A*, Immunostaining of the rosette-like structure with anti-nestin (primary antibody); it was incubated with secondary antibody and counterstained with ethidium bromide. *B*, A phase contrast image of *A*. *C*, Immunostaining of the rosette-like structure with anti-neurofilament 68 (primary antibody); it was incubated with secondary antibody and counterstained with ethidium bromide. *D*, A phase contrast image of *B*. *E*, The immunostaining of the neural stem cells in the rosette-like structure with anti-N-cadherin antibody, which was (primary antibody) followed by incubation with secondary antibody conjugated with FITC and counterstained with ethidium bromide. *F*, A phase contrast image of *E* (*scale bar*= 500 µm).

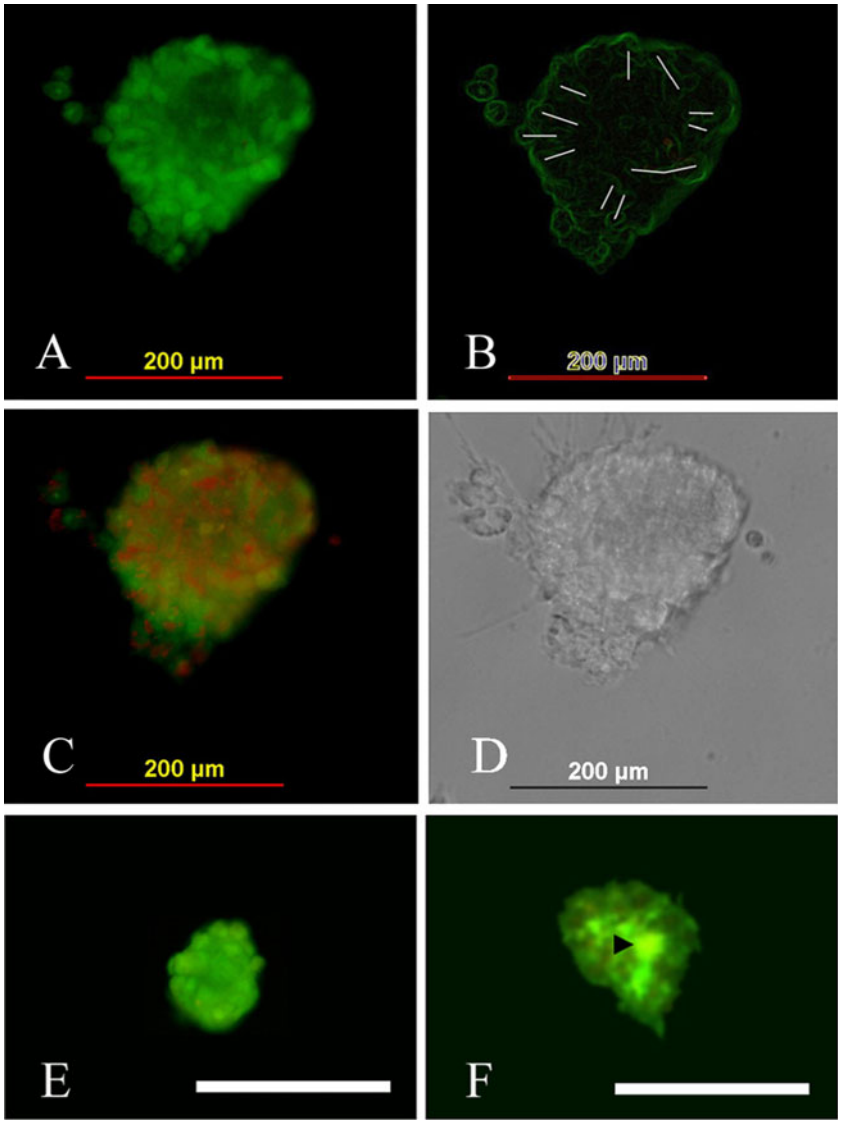

Figure 7. The immunostaining of the neurospheres with the adhesion molecule (N-cadherin). *A*, A neurosphere stained with acridine orange used as a background for the immunostaining of N-cadherin. *B*, The image in *A* subjected to image processing including increase contrast and edge detection using Image J software (NIH); the edge of the cells in the neurosphere shows that the cells at the margin of the neurosphere tend to form linear patterns with an arrangement of radial-like formation. *C*, The double staining of a neurosphere with acridine orange; it was the labeled with anti-N-cadherin antibody (primary antibody) then incubated with secondary antibody conjugated with Alexa Flour (*red* fluorescence). *D*, A phase contrast of *A*, *B*, and *C*. *E*, Staining of the neurospheres with acridine orange then immunostained with anti-Neu N (primary antibody) and it was incubated with secondary antibody conjugated with Alexa Fluor (*red*). *F*, Staining of the neurospheres with acridine orange then immunostained with anti-GFAP (primary antibody) and it was incubated with secondary antibody conjugated with Alexa Fluor; *arrowhead* indicates the site of immunoreactive cells (*scale bar*= 200 µm, *E* and *F*).

significantly higher than the other markers. Among the neurofilaments, the percentage of the cells immunoreactive to NF68 was significantly higher than that of NF160 and NF200, and its value in NF160 was significantly higher than in NF200 (Fig. 4*C*) ($P<0.05$). GFAP was significantly lower than the other neuronal markers except NF200 ($P<0.05$).

Within 1 d, the cultured cells in the suspension medium (harvested from the neurospheres) were round with eccentric nuclei and forming typical polarized cells (Fig. 5*A*). Moreover, staining these cells with acridine orange resulted in either red color (postmitotic/presynthetic phase of cell cycle, PM) or green color (premitotic/postsynthetic phase of cell cycle, PS). Few cells were aggregated forming the initial neurosphere, and subsequently more cell aggregates could be seen (4 h) (Fig. 5*B*). Some of the aggregated cells had a synchronized phase (all of the cells at the single phase of the cell cycle), while the others were at mixed phases of the cell cycle (see Fig. 5*C*, *D*, *E*, *F*; at days 1, 1, 4, and 4, respectively). Few polarized cells were arranged in special pattern with their nuclei interphasing each other forming a primitive rosette-like structure, and they synchronized in their cell cycle (see Fig. 5*C*, *D*). Moreover, the neurospheres were formed from aggregation of the polarized cells, and when the neurospheres were maintained for a longer time in the culturing system, they consisted of a mixture of PM and PS. Some neurospheres were engaged in fusion activity (Fig. 5*F*).

When the NSCs in the neurospheres were cultured on adherent plates, the cells tended to form isolated aggregates with more cells accumulated at the center of the aggregate in a pattern similar to a rosette (rosette-like structure), either single (Fig. 6*A–D*), double (Figs. 5*E*, *F* and 6*E*, *F*), or multiple rosette-like (Fig. 7*E*, *F*). Immunostaining of the cells in the rosette-like structure showed immunoreactivity to nestin, NF68, and N-cadherin (Fig. 6*A*, *C*, *E*). Figure 7 (*A–D*) represents staining of a neurosphere with acridine

orange (A: green fluorescence) followed by immunostaining with N-cadherin. Image processing of the acridine orange stained image by increasing contrast and edge detection softwares (Image J, NIH) showed that the cells in the submarginal region tended to align linearly with the outer marginal cells forming a radiating pattern similar to rosettes; however, the lumen was not yet formed (Fig. 7*B*). Most of the cells forming the neurosphere were immunoreactive to N-cadherin (Fig. 7*C*). Figure 8 shows a neurosphere stained with acridine orange followed by ethidium bromide, the image was processed using Image J software (NIH), and the image color was spilt into blue, green, and red colors. The red color showed the nuclei of the cells at the top of the sphere arranged in a radial-like pattern; the edge detection of the image showed a consistent pattern. The neurospheres showed no immunoreactivity to Neu N and few cells immunoreactivity to GFAP (see Fig. 7*E*, *F*, respectively). The molecular profile of the BMSCs, the neurospheres, and the NSCs using RT-PCR was used in evaluating the pluripotency genes SOX2, OCT4, and Nanog. The results show that the BMSCs expressed Oct4 and Nanog; however, in the neurospheres, Oct4 and SOX2 were expressed but Nanog was repressed, while in the NSCs, only SOX2 gene was expressed (see Fig. 9). Another pluripotency gene (c-Myc) was assessed by immunocytochemistry, and c-Myc protein was expressed in BMSCs, NS, and NSCs (Fig. 10). The expression profile of the differentiation genes (NeuroD1, GFAP, fibronectin, tubulin β4, nestin, MBP, and Musashi I) is presented in Fig. 9.

Discussion

In this study, the suspended NSCs had polar morphology expressed the pluripotency genes SOX2 and c-Myc and the neural stem cell genes nestin, NeuroD1, and Musashi I. The polarized cells formed rosette-like structures when they were cultured in suspension medium under adherent condition.

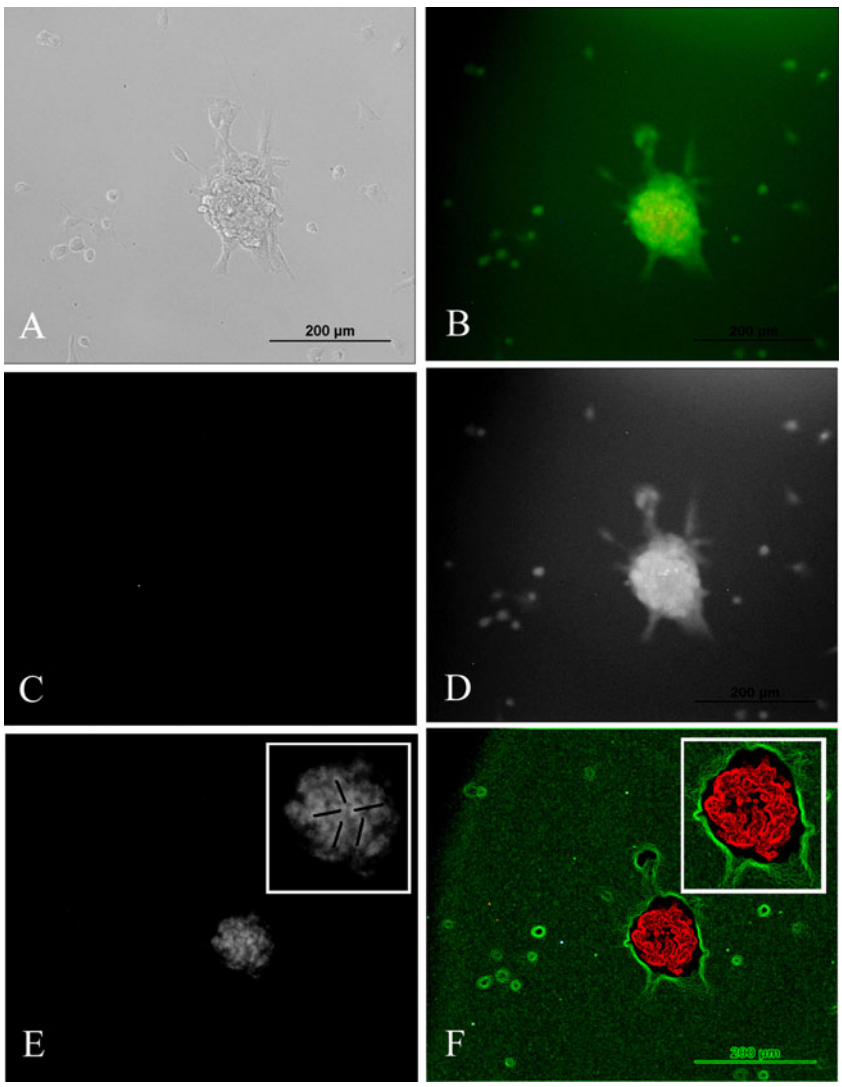

Figure 8. Double staining of a neurosphere with acridine orange followed by staining with ethidium bromide; the image was processed using image J software (NIH). *A*, A phase image of the neurosphere. *B*, A neurosphere stained with acridine orange followed by staining with ethidium bromide. *C*, The double-stained neurosphere image processed with image spilt command, *blue color* split; *D*, *E*, The *green* and *red ones*, respectively; *inset* in *E* shows higher resolution image of *red color* regions (nuclei) with tendency to form linear patterns with an arrangement of radial-like formation. *Insets* in *F* shows the pattern of the cells in edge find command at a higher resolution; the cells tend to form radial pattern toward the center.

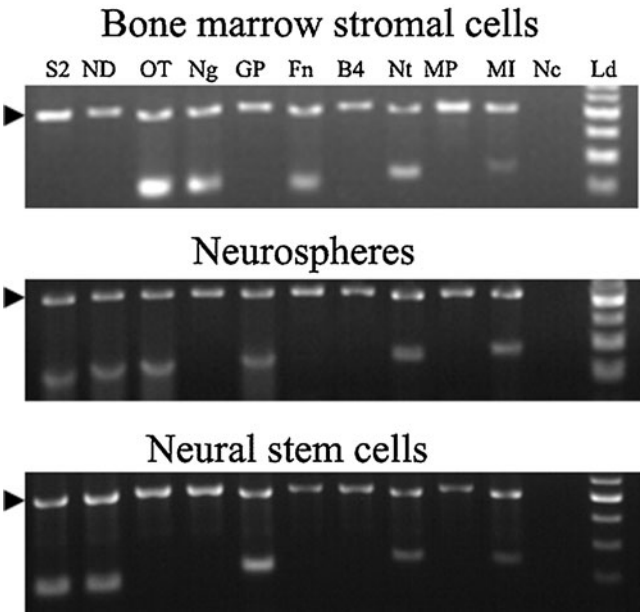

Figure 9. Electrophorograms of RT-PCR products for SOX2 (*S2*), NeuroD1 (*ND*), OCT4 (*OT*), Nanog (*Ng*), GFAP (*GP*), fibronectin (*Fn*), tubb4 (*B4*), nestin (*Nt*), MBP (*MP*), and Musashi I (*MI*) genes, using the mRNAs extracted from the bone marrow stromal cells, neurospheres, and neural stem cells at the *upper*, *middle*, and *lower panels*, respectively. Nc and Ld represent the negative control and the ladder, respectively. *Arrowhead* indicates the bands of the housekeeping gene (internal control): glyceraldehyde 3-phosphate dehydrogenase 496 bp.

The BMSCs were derived from mesodermal lineages, confirmed by the lipogenic as well as osteogenic induction and by the markers of the cells, which is consistent with the findings of the others (Mohammad-Gharibani et al. 2012). The cells expressed Oct4, a pluripotency gene. Sterneckert et al. (2012) reported that introducing Oct4 into cells could result in its reprogramming and transdifferentiation into another lineage such as neural phenotype. Warthemann et al. (2012) reported that the Oct4a was more important variant in the pluripotency than Oct4b. Oct4a was reported to be an important stemness gene in the derivation of neural lineages (Parte et al. 2011). In this study, the antibody selected was immunoreactive to Oct4a because the commercial source is important in detecting this marker (Zuk 2009). Moreover, a decline in Oct4 expression was noticed with the incubation of BMSCs with combined EGF/bFGF. Delcroix et al. (2010) reported a decrease in Oct4 and the expression of cell cycle control genes, and increase in expression of neural differentiation genes. For example, using a low dose of 5–10 ng/ml (both EGF/bFGF) resulted in approximately a three-fold increase in the expression of nestin, which did not show further increase with higher dose (50 ng/ml). On the one hand, in this study, the cells in the neurospheres showed positive immunostaining with nestin, but they were not immunoreactive to Neu N because it is a differentiated neuron marker (Lu et al. 2003); on the other hand, the immunostaining of BMSCs-derived NSCs showed that most of the cells were immunoreactive to nestin, which is consistent with the percentage of immunoreactive cells to this marker, while similar results were noticed in immunostaining with GFAP. Moreover, only few cells in the neurospheres were immunoreactive to GFAP. The marker of oligodendrocyte (O4) showed that few cells had positive reactivity, which is consistent with a previous finding (Kaka et al. 2012). This indicated that the BMSCs are multipotent stem cells (Liu et al. 2006).

Acridine orange is a differential nuclear DNA dye, which stains nuclear DNA green under a fluorescent microscope, while the RNA in the cytoplasm of the cells engaged in protein synthesis shows red fluorescent color (Nicolini et al. 1979); at the PS, the color is essentially green (Traganos et al. 1977). Also, Alam et al. (2004) documented that there is staining difference between RNA and DNA, the cell cycle phase either pre-DNA or post-DNA synthesis, which could be used for analyzing its G1, S, and G2+M progression (Darzynkiewicz et al. 1976). In our experiment, we used acridine orange for evaluating the neurosphere-forming cells and the suspended NSCs at either PS or PM. This staining showed that the NSCs in the suspension medium were polarized; the same feature was seen in the developing embryo (Farkas and Huttner 2008). The interesting result of the staining with acridine orange was the synchronization of the NSCs (all of them at PM) into a rosette-like structure, which may arose from the expression of similar proteins in the synchronized cells (Uzbekov 2004; Bianchi 2008; Banfalvi 2011), such as the adhesion molecules (Becker et al. 1999; Klein et al. 2007); this is consistent with N-cadherin immunostaining of the neurospheres.

The harvested neurospheres yielded uniform polarized cells (apical nucleus with apicobasal polarity), which were documented to differentiate into several types of cells in the developing central nervous system (Gotz and Huttner 2005). Cell polarity was described in in vivo studies; for example, Kumar et al. (2011) denoted that cell polarization had a feature of geometry-based orientation, which is important in cell motion during fetal neurogenesis, a major factor in the nervous system morphogenesis. Moreover, a living imaging experiment showed that the cell group polarity is important for directional migration forming a correct three-dimensional geometry during the central nervous system organogenesis resulting in the functional structure (Aman and Piotrowski 2010). On the one hand, in the developing nervous system, the polarized neuroepithelial cells contain neural stem cells, which is essential for generating the neuroglial cells (Wakamatsu et al. 2007). On the other hand, the importance of polarity is considered a key feature in the proliferation/differentiation of the neuroepithelial cells in the developing rodent neocortex (Farkas and Huttner 2008); this was also reported in the neural tube, where the

apicobasal polarity of neuroepithelium is an important characteristic of the differentiating cells (Wilson and Stice 2006).

In vitro studies on embryonic carcinoma cells showed that the cells forming the rosette structure had polar morphology (Finley et al. 1996); in addition, other investigators disclosed that human embryonic stem cell-derived rosettes were initiated by polarized cells (Elkabetz et al. 2008). Ma et al. (1998) defined the rosette-like structure as spreading of the cells from the edge of the neurosphere attached to an adherent surface, and the source was fetal neuroepithelium dissected from the rat embryo. Rosette-like structures were also derived from adult stem cells such as adipose derived stem cells cultured for long term without supplementation resulting in spontaneous differentiation with rosette-like formation; however, the neural differentiation efficiency was low with significant cell death (Qian et al. 2010). In this study, the rosette-like structures were derived from neurospheres formed from BMSCs with multiple adherent rosettes-like structures, where the cells were radiating out of the clusters; similar architecture was noticed in human embryonic stem cells (Bajpai et al. 2009), but generation of rosette structures from adult neural tissues was rarely documented (Podgornyi et al. 2005).

In our investigation, the c-Myc (a pluripotency gene) was expressed in BMSCs, neurospheres, and NSCs, while other pluripotency genes showed transcriptional changes, characterized by gene switching, either gradual (decline: Oct4 and increase: SOX2) or abrupt shut down (Nanog). This may represent the existence of a defined regulatory network in BMSC differentiation into NSCs. In the BMSCs, the expression of Oct4 and Nanog was detected, this is consistent with the pluripotency gene expression in hESCs and mESCs, and both Oct4 and Nanog contributed to the expression of SOX2 (Loh et al. 2006) in NSCs (Plane et al. 2012). Boyer et al. (2005) reported that the pluripotency genes (Nanog, OCT4, and SOX2) could induce the expression of NeuroD1, which is an important regulatory factor in neurogenesis.

The expression of c-Myc was documented in BMSCs (Kim et al. 2007); neurospheres (Narayanan et al. 2012), which increased self-renewal in neural progenitor cells (Kerosuo et al. 2008); and NSCs, where c-Myc acted as a transcriptional cofactor (Martínez-Cerdeño et al. 2012). The expression of Oct4 was consistently noticed in BMSCs (Ren et al. 2006; Cui et al. 2009) and neurospheres (Singh et al. 2009), but not in NSCs (Daadi et al. 2008). Nanog

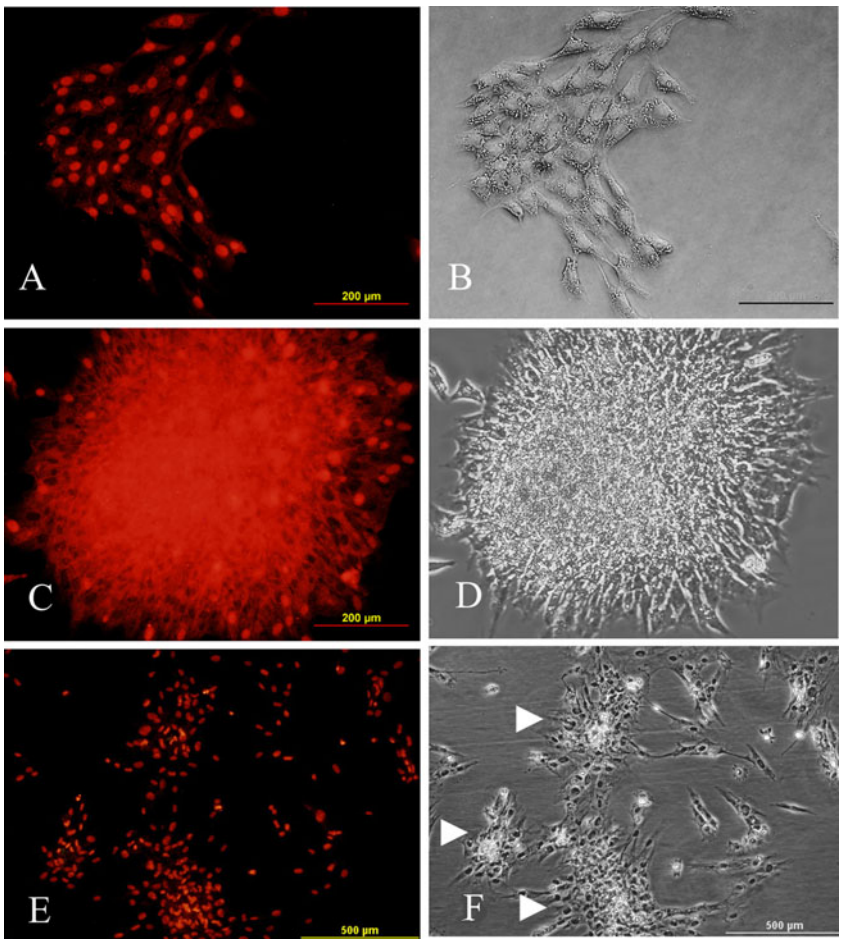

Figure 10. The immunostaining of bone marrow stromal cells (BMSCs), neurosphere (NS), and neural stem cells (NSCs) with anti-c-Myc antibody. *A*, The immunostaining of BMSCs with anti-c-Myc antibody (primary antibody), which was followed by incubation with secondary antibody conjugated with Alexa Fluor (*red* fluorescence). *B*, A phase contrast image of *A*. *C*, The immunostaining of NS with anti-c-Myc antibody (primary antibody) which was followed by incubation with secondary antibody conjugated with Alexa Fluor (*red* fluorescence). *D*, A phase contrast image of *C*. *E*, The immunostaining of the rosette-like structures in the adherent culture with anti-c-Myc antibody (primary antibody), which was followed by incubation with secondary antibody conjugated with Alexa Fluor (red fluorescence). *F*, A phase contrast image of *E*.

expression was confirmed in BMSCs (Esposito et al. 2009), though its expression in NSCs was not detected (Sundberg et al. 2011). SOX2 was expressed in neurospheres (Zheng et al. 2011) and NSCs (Plane et al. 2012), but not detected in BMSCs (Riekstina et al. 2009); SOX2 was universally known as a marker of neural progenitor and NSCs throughout the vertebrate CNS (Uwanogho et al. 1995; Graham et al. 2003; Techawattanawisal et al. 2007). On the one hand, NeuroD1, a transcription factor in early neuron differentiation (Roybon et al. 2010), was not expressed in BMSCs but in neurospheres (Hermann et al. 2004) as well as NSCs (Franklin et al. 2001; Bertrand et al. 2002). Similar results were noticed with GFAP (Hermann et al. 2004; Streckfuss-Bömeke et al. 2009). The reverse was noticed in the expression of fibronectin, a BMSCs marker (Hermann et al. 2004). On the other hand, MBP, expressed in myelin sheath-forming oligodendrocytes, showed results which agree with previous investigations (Hermann et al. 2004; Fulton et al. 2010; Mekhail et al. 2012), so did Tubb4, a specific marker for differentiated neurons (Hermann et al. 2004; Streckfuss-Bömeke et al. 2009). Musashi I showed a reverse pattern of expression, where the gene was expressed in NS and NSCs, which coincides with previous findings (Sakakibara et al. 1996; Kaneko et al. 2000; Keyoung et al. 2001). In this study, Musashi I mRNA was also detected in BMSCs, which is consistent with other investigation (Okumoto et al. 2005; Valcz et al. 2011).

In our investigation, nestin immunoreactive cells were noticed in neurospheres and NSCs, as reported by the others (Mothe et al. 2011; Sun et al. 2011); Bazán et al. (2004) considered nestin as a key marker in NSCs in both in vitro and in vitro conditions. However, we detected nestin mRNA in the BMSCs, while nestin immunostaining was not, which may be due to a post-transcriptional control which did not allow the translation of mRNA (Movaghar et al. 2008); moreover, Binello et al. (2012) considered nestin as a stemness marker which could be expressed by BMSCs.

Neurosphere-forming cells were immunostained for N-cadherin; this finding was documented by Kim et al. (2010) and Lobo et al. (2003). While N-cadherin expression was noticed in the ESC-generated rosettes, it was observed at the apical part of the cells surrounding the lumen (Pankratz et al. 2007). Our results show that the cells of the neurosphere were more uniformly immunostained with N-cadherin but the lumen was not yet evolved and the cells were inclined to arrange linearly toward the center (see Fig. 7*A–D*); this may indicate the tendency of the neurospheres derived from the BMSCs to form a rosette. The results of N-cadherin expression in NSCs agree with previous investigations (Curchoe et al. 2010; Kim et al. 2010). Moreover, image processing of a double-stained neurosphere with acridine orange and ethidium bromide showed consistent arrangement of the ethidium bromide nuclei forming radial-like patterns.

Conclusions

The NSCs generated from BMSC-derived neurospheres have the morphology and the characteristics of neuroepithelial cells with tendency to forming rosette-like structures.

Acknowledgments The project was funded by Shefa Neurosciences Research Center at Khatam Al-Anbia Hospital, Tehran, Iran (grant # 86-N-105). We are also grateful for the support of the Faculty of Medical Sciences, Tarbiat Modares University, Tehran, Iran. We are grateful for Mrs. Hanna A, Akbar for assistance in editing the manuscript.

References

Abdanipour A.; Tiraihi T.; Delshad A. Trans-differentiation of the adipose tissue-derived stem cells into neuron-like cells expressing neurotrophins by selegiline. *Iran Biomed J* 15(4): 113–121; 2011a.

Abdanipour A.; Tiraihi T.; Mirnajafi-Zadeh J. Improvement of the pilocarpine epilepsy model in rat using bone marrow stromal cell therapy. *Neurol Res* 33(6): 625–632; 2011b.

Alam S.; Sen A.; Behie L. A.; Kallos M. S. Cell cycle kinetics of expanding populations of neural stem and progenitor cells in vitro. *Biotechnol Bioeng* 88(3): 332–347; 2004.

Aman A.; Piotrowski T. Cell migration during morphogenesis. *Dev Biol* 341: 20–33; 2010.

Bajpai R.; Coppola G.; Kaul M.; Talantova M.; Cimadamore F.; Nilbratt M.; Geschwind D. H.; Lipton S. A.; Terskikh A. V. Molecular stages of rapid and uniform neutralization of human embryonic stem cells. *Cell Death Differ* 16(6): 807–825; 2009.

Banfalvi G. Overview of cell synchronization. *Methods Mol Biol* 761: 1–23; 2011.

Barnabé G. F.; Schwindt T. T.; Calcagnotto M. E.; Motta F. L.; Martinez Jr. G.; de Oliveira A. C.; Keim L. M.; D'Almeida V.; Mendez-Otero R.; Mello L. E. Chemically-induced RAT mesenchymal stem cells adopt molecular properties of neuronal-like cells but do not have basic neuronal functional properties. *PLoS One* 4(4): e52; 2009.

Bazán E.; Alonso F. J.; Redondo C.; López-Toledano M. A.; Alfaro J. M.; Reimers D.; Herranz A. S.; Paíno C. L.; Serrano A. B.; Cobacho N.; Caso E.; Lobo M. V. In vitro and in vivo characterization of neural stem cells. *Histol Histopathol* 19(4): 1261–1752; 2004.

Becker P. S.; Nilsson S. K.; Li Z.; Berrios V. M.; Dooner M. S.; Cooper C. L.; Hsieh C. C.; Quesenberry P. J. Adhesion receptor expression by hematopoietic cell lines and murine progenitors: modulation by cytokines and cell cycle status. *Exp Hematol* 27(3): 533–541; 1999.

Bertrand N.; Castro D. S.; Guillemot F. Proneural genes and the specification of neural cell types. *Nat Rev Neurosci* 3(7): 517–30; 2002.

Bianchi M. M. Collective behavior in gene regulation: metabolic clocks and cross-talking. *FEBS J* 275(10): 2356–2363; 2008.

Binello E.; Qadeer Z. A.; Kothari H. P.; Emdad L.; Germano I. M. Stemness of the CT-2A immunocompetent mouse brain tumor model: characterization in vitro. *J Cancer* 3: 166–174; 2012.

Boyer L. A.; Lee T. I.; Cole M. F.; Johnstone S. E.; Levine S. S.; Zucker J. P.; Guenther M. G.; Kumar R. M.; Murray H. L.; Jenner R. G.; Gifford D. K.; Melton D. A.; Jaenisch R.; Young R. A. Core transcriptional regulatory circuitry in human embryonic stem cells. *Cell* 122(6): 947–56; 2005.

Chen Y.; Teng F. Y.; Tang B. L. Coaxing bone marrow stromal mesenchymal stem cells towards neuronal differentiation: progress and uncertainties. *Cell Mol Life Sci* 63(14): 1649–1657; 2006.

Croft A. P.; Przyborski S. A. Generation of neuroprogenitor-like cells from adult mammalian bone marrow stromal cells in vitro. *Stem Cells Dev* 13(4): 409–420; 2004.

Cui G.; Qi Z.; Guo X.; Qin J.; Gui Y.; Cai Z. Rat bone marrow derived mesenchymal progenitor cells support mouse ES cell growth and germ-like cell differentiation. *Cell Biol Int* 33(3): 434–441; 2009.

Curchoe C. L.; Maurer J.; McKeown S. J.; Cattarossi G.; Cimadamore F.; Nilbratt M.; Snyder E. Y.; Bronner-Fraser M.; Terskikh A. V. Early acquisition of neural crest competence during hESCs neuralization. *PLoS One* 5(11): e13890; 2010.

Daadi M. M.; Maag A. L.; Steinberg G. K. Adherent self-renewable human embryonic stem cell-derived neural stem cell line: functional engraftment in experimental stroke model. *PLoS One* 3(2): e1644; 2008.

Darzynkiewicz Z.; Traganos F.; Sharpless T.; Melamed M. R. Lymphocyte stimulation: a rapid multiparameter analysis. *Proc Natl Acad Sci USA* 73(8): 2881–2884; 1976.

Delcroix G. J.; Curtis K. M.; Schiller P. C.; Montero-Menei C. N. EGF and bFGF pre-treatment enhances neural specification and the response to neuronal commitment of MIAMI cells. *Differentiation* 80: 213–227; 2010.

Deng W.; Obrocka M.; Fischer I.; Prockop D. J. In vitro differentiation of human marrow stromal cells into early progenitors of neural cells by conditions that increase intracellular cyclic AMP. *Biochem Biophys Res Commun* 282(1): 148–152; 2001.

Dezawa M.; Kanno H.; Hoshino M.; Cho H.; Matsumoto N.; Itokazu Y.; Tajima N.; Yamada H.; Sawada H.; Ishikawa H.; Mimura T.; Kitada M.; Suzuki Y.; Ide C. Specific induction of neuronal cells from bone marrow stromal cells and application for autologous transplantation. *J Clin Invest* 113(12): 1701–1710; 2004.

Elkabetz Y.; Panagiotakos G.; Al Shamy G.; Socci N. D.; Tabar V.; Studer L. Human ES cell-derived neural rosettes reveal a functionally distinct early neural stem cell stage. *Genes Dev* 22(2): 152–165; 2008.

Esposito M. T.; Di Noto R.; Mirabelli P.; Gorrese M.; Parisi S.; Montanaro D.; Del Vecchio L.; Pastore L. Culture conditions allow selection of different mesenchymal progenitors from adult mouse bone marrow. *Tissue Eng Part A* 15(9): 2525–2536; 2009.

Farkas L. M.; Huttner W. B. The cell biology of neural stem and progenitor cells and its significance for their proliferation versus differentiation during mammalian brain development. *Curr Opin Cell Biol* 20(6): 707–715; 2008.

Finley M. F.; Kulkarni N.; Huettner J. E. Synapse formation and establishment of neuronal polarity by P19 embryonic carcinoma cells and embryonic stem cells. *J Neurosci* 16(3): 1056–1065; 1996.

Franklin A.; Kao A.; Tapscott S.; Unis A. NeuroD homologue expression during cortical development in the human brain. *J Child Neurol* 16(11): 849–53; 2001.

Fulton D.; Paez P. M.; Campagnoni A. T. The multiple roles of myelin protein genes during the development of the oligodendrocyte. *ASN Neuro* 2(1): e00027; 2010.

Ge Y.; Zhou F.; Chen H.; Cui C.; Liu D.; Li Q.; Yang Z.; Wu G.; Sun S.; Gu J.; Wei Y.; Jiang J. Sox2 is translationally activated by eukaryotic initiation factor 4E in human glioma-initiating cells. *Biochem Biophys Res Commun* 397(4): 711–717; 2010.

Ghorbanian M. T.; Tiraihi T.; Mesbah-Namin S. A.; Fathollahi Y. Selegiline is an efficient and potent inducer for bone marrow stromal cell differentiation into neuronal phenotype. *Neurol Res* 32(2): 185–193; 2010.

Gotz M.; Huttner W. B. The cell biology of neurogenesis. *Mol Cell Biol* 6: 777–788; 2005.

Graham V.; Khudyakov J.; Ellis P.; Pevny L. SOX2 functions to maintain neural progenitor identity. *Neuron* 39(5): 749–765; 2003.

Hellmann M. A.; Panet H.; Barhum Y.; Melamed E.; Offen D. Increased survival and migration of engrafted mesenchymal bone marrow stem cells in 6-hydroxydopamine-lesioned rodents. *Neurosci Lett* 395(2): 124–128; 2006.

Hermann A.; Gastl R.; Liebau S.; Popa M. O.; Fiedler J.; Boehm B. O.; Maisel M.; Lerche H.; Schwarz J.; Brenner R.; Storch A. Efficient generation of neural stem cell-like cells from adult human bone marrow stromal cells. *J Cell Sci* 117(Pt 19): 4411–4422; 2004.

Hung S. C.; Cheng H.; Pan C. Y.; Tsai M. J.; Kao L. S.; Ma H. L. In vitro differentiation of size-sieved stem cells into electrically active neural cells. *Stem Cells* 20(6): 522–529; 2002.

Kaka G. R.; Tiraihi T.; Delshad A.; Arabkheradmand J.; Kazemi H. In vitro differentiation of bone marrow stromal cells into oligodendrocyte-like cells using triiodothyronine as inducer. *Int J Neurosci* 122(5): 237–247; 2012.

Kaneko Y.; Sakakibara S.; Imai T.; Suzuki A.; Nakamura Y.; Sawamoto K.; Ogawa Y.; Toyama Y.; Miyata T.; Okano H. Musashi1: an evolutionally conserved marker for CNS progenitor cells including neural stem cells. *Dev Neurosci* 22(1–2): 139–153; 2000.

Kerosuo L.; Piltti K.; Fox H.; Angers-Loustau A.; Häyry V.; Eilers M.; Sariola H.; Wartiovaara K. Myc increases self-renewal in neural progenitor cells through Miz-1. *J Cell Sci* 121(Pt 23): 3941–3950; 2008.

Keyoung H. M.; Roy N. S.; Benraiss A.; Louissaint Jr. A.; Suzuki A.; Hashimoto M.; Rashbaum W. K.; Okano H.; Goldman S. A. High-yield selection and extraction of two promoter-defined phenotypes of neural stem cells from the fetal human brain. *Nat Biotechnol* 19(9): 843–850; 2001.

Kim M. S.; Shin Y. N.; Cho M. H.; Kim S. H.; Kim S. K.; Cho Y. H.; Khang G.; Lee I. W.; Lee H. B. Adhesion behavior of human bone marrow stromal cells on differentially wettable polymer surfaces. *Tissue Eng* 13(8): 2095–2103; 2007.

Kim M. Y.; Kaduwal S.; Yang D. H.; Choi K. Y. Bone morphogenetic protein 4 stimulates attachment of neurospheres and astrogenesis of neural stem cells in neurospheres via phosphatidylinositol 3 kinase-mediated upregulation of N-cadherin. *Neuroscience* 170(1): 8–15; 2010.

Klein E. A.; Yung Y.; Castagnino P.; Kothapalli D.; Assoian R. K. Cell adhesion, cellular tension, and cell cycle control. *Methods Enzymol* 426: 155–175; 2007.

Kohyama J.; Abe H.; Shimazaki T.; Koizumi A.; Nakashima K.; Gojo S.; Taga T.; Okano H.; Hata J.; Umezawa A. Brain from bone: efficient "meta-differentiation" of marrow stroma-derived mature osteoblasts to neurons with Noggin or a demethylating agent. *Differentiation* 68(4–5): 235–244; 2001.

Kumar G.; Co C. C.; Ho C. C. Steering cell migration using microarray amplification of natural directional persistence. *Langmuir* 27(7): 3803–3807; 2011.

Levy Y. S.; Merims D.; Panet H.; Barhum Y.; Melamed E.; Offen D. Induction of neuron-specific enolase promoter and neuronal markers in differentiated mouse bone marrow stromal cells. *J Mol Neurosci* 21(2): 121–132; 2003.

Li Y.; Chen J.; Wang L.; Lu M.; Chopp M. Treatment of stroke in rat with intracarotid administration of marrow stromal cells. *Neurology* 56(12): 1666–1672; 2001.

Liu W.; Cui L.; Cao Y. Bone reconstruction with bone marrow stromal cells. *Methods Enzymol* 420: 362–80; 2006.

Lobo M. V.; Alonso F. J.; Redondo C.; López-Toledano M. A.; Caso E.; Herranz A. S.; Paíno C. L.; Reimers D.; Bazán E. Cellular characterization of epidermal growth factor-expanded free-floating neurospheres. *J Histochem Cytochem* 51(1): 89–103; 2003.

Loh Y. H.; Wu Q.; Chew J. L.; Vega V. B.; Zhang W.; Chen X.; Bourque G.; George J.; Leong B.; Liu J.; Wong K. Y.; Sung K. W.; Lee C. W.;

Zhao X. D.; Chiu K. P.; Lipovich L.; Kuznetsov V. A.; Robson P.; Stanton L. W.; Wei C. L.; Ruan Y.; Lim B.; Ng H. H. The Oct 4 and Nanog transcription network regulates pluripotency in mouse embryonic stem cells. *Nat Genet* 38(4): 431–40; 2006.

Lu D.; Mahmood A.; Wang L.; Li Y.; Lu M.; Chopp M. Adult bone marrow stromal cells administered intravenously to rats after traumatic brain injury migrate into brain and improve neurological outcome. *Neuroreport* 12(3): 559–563; 2001.

Lu P.; Blesch A.; Tuszynski M. H. Induction of bone marrow stromal cells to neurons: differentiation, transdifferentiation, or artifact? *J Neurosci Res* 77(2): 174–191; 2004.

Lu P.; Jones L. L.; Snyder E. Y.; Tuszynski M. H. Neural stem cells constitutively secrete neurotrophic factors and promote extensive host axonal growth after spinal cord injury. *Exp Neurol* 181(2): 115–129; 2003.

Ma W.; Liu Q. Y.; Maric D.; Sathanoori R.; Chang Y. H.; Barker J. L. Basic FGF-responsive telencephalic precursor cells express functional GABA(A) receptor/Cl-channels in vitro. *J Neurobiol* 35(3): 277–286; 1998.

Martínez-Cerdeño V.; Lemen J. M.; Chan V.; Wey A.; Lin W.; Dent S. R.; Knoepfler P. S. N-Myc and GCN5 regulate significantly overlapping transcriptional programs inneural stem cells. *PLoS One* 7(6): e39456; 2012.

Mekhail M.; Almazan G.; Tabrizian M. Oligodendrocyte-protection and remyelination post-spinal cord injuries: a review. *Prog Neurobiol* 96(3): 322–339; 2012.

Mohammad-Gharibani P.; Tiraihi T.; Mesbah-Namin S. A.; Arabkheradmand J.; Kazemi H. Induction of bone marrow stromal cells into GABAergic neuronal phenotype using creatine as inducer. *Restor Neurol Neurosci* 30(6): 511–525; 2012.

Mothe A. J.; Zahir T.; Santaguida C.; Cook D.; Tator C. H. Neural stem/progenitor cells from the adult human spinal cord are multipotent and self-renewing and differentiate after transplantation. *PLoS One* 6(11): e27079; 2011.

Movaghar B.; Tiraihi T.; Mesbah-Namin S. A. Transdifferentiation of bone marrow stromal cells into Schwann cell phenotype using progesterone as inducer. *Brain Res* 1208: 17–24; 2008.

Narayanan G.; Poonepalli A.; Chen J.; Sankaran S.; Hariharan S.; Yu Y. H.; Robson P.; Yang H.; Ahmed S. Single-cell mRNA profiling identifies progenitor subclasses in neurospheres. *Stem Cells Dev* 21(18): 3351–3362; 2012.

Neuhuber B.; Gallo G.; Howard L.; Kostura L.; Mackay A.; Fischer I. Reevaluation of in vitro differentiation protocols for bone marrow stromal cells: disruption of actin cytoskeleton induces rapid morphological changes and mimics neuronal phenotype. *J Neurosci Res* 77(2): 192–204; 2004.

Nicolini C.; Belmont A.; Parodi S.; Lessin S.; Abraham S. Mass action and acridine orange staining: static and flow cytofluorometry. *J Histochem Cytochem* 27(1): 102–113; 1979.

Okumoto K.; Saito T.; Hattori E.; Ito J. I.; Suzuki A.; Misawa K.; Sanjyo M.; Takeda T.; Sugahara K.; Saito K.; Togashi H.; Kawata S. Expression of Notch signalling markers in bone marrow cells that differentiate into a liver cell lineage in a rat transplant model. *Hepatol Res* 31(1): 7–12; 2005.

Pankratz M. T.; Li X. J.; Lavaute T. M.; Lyons E. A.; Chen X.; Zhang S. C. Directed neural differentiation of human embryonic stem cells via an obligated primitive anterior stage. *Stem Cells* 25(6): 1511–1520; 2007.

Parte S.; Bhartiya D.; Telang J.; Daithankar V.; Salvi V.; Zaveri K.; Hinduja I. Detection, characterization, and spontaneous differentiation in vitro of very small embryonic-like putative stem cells in adult mammalian ovary. *Stem Cells Dev* 20(8): 1451–1464; 2011.

Plane J. M.; Grossenbacher S. K.; Deng W. PARP-1 deletion promotes subventricular zone neural stem cells toward a glial fate. *J Neurosci Res* 90(8): 1489–1506; 2012.

Podgornyi O. V.; Poltavtseva R. A.; Marei M. V.; Sukhikh G. T.; Aleksandrova M. A. Formation of neuroepithelial structures in culture of neural stem cells from human brain. *Bull Exp Biol Med* 140(1): 113–117; 2005.

Qian D. X.; Zhang H. T.; Ma X.; Jiang X. D.; Xu R. X. Comparison of the efficiencies of three neural induction protocols in human adipose stromal cells. *Neurochem Res* 35(4): 572–579; 2010.

Rao V. S.; Carvalho A. C.; Trevisan M. T.; Andrade G. M.; Nobre-Júnior H. V.; Moraes M. O.; Magalhães H. I.; Morais T. C.; Santos F. A. Mangiferin ameliorates 6-hydroxydopamine-induced cytotoxicity and oxidative stress in ketamine model of schizophrenia. *Pharmacol Rep* 64(4): 848–856; 2012.

Ren H.; Cao Y.; Zhao Q.; Li J.; Zhou C.; Liao L.; Jia M.; Zhao Q.; Cai H.; Han Z. C.; Yang R.; Chen G.; Zhao R. C. Proliferation and differentiation of bone marrow stromal cells under hypoxic conditions. *Biochem Biophys Res Commun* 347(1): 12–21; 2006.

Reynolds B. A.; Weiss S. Generation of neurons and astrocytes from isolated cells of the adult mammalian central nervous system. *Science* 255(5052): 1707–1710; 1992.

Riekstina U.; Cakstina I.; Parfejevs V.; Hoogduijn M.; Jankovskis G.; Muiznieks I.; Muceniece R.; Ancans J. Embryonic stem cell marker expression pattern in human mesenchymal stem cells derived from bone marrow, adipose tissue, heart and dermis. *Stem Cell Rev* 5(4): 378–386; 2009.

Roybon L.; Mastracci T. L.; Ribeiro D.; Sussel L.; Brundin P.; Li J. Y. GABAergic differentiation induced by Mash1 is compromised by the bHLH proteins Neurogenin2, NeuroD1, and NeuroD2. *Cereb Cortex* 20(5): 1234–1244; 2010.

Sakakibara S.; Imai T.; Hamaguchi K.; Okabe M.; Aruga J.; Nakajima K.; Yasutomi D.; Nagata T.; Kurihara Y.; Uesugi S.; Miyata T.; Ogawa M.; Mikoshiba K.; Okano H. Mouse-Musashi-1, a neural RNA-binding protein highly enriched in the mammalian CNS stem cell. *Dev Biol* 176(2): 230–242; 1996.

Sanchez-Ramos J.; Song S.; Cardozo-Pelaez F.; Hazzi C.; Stedeford T.; Willing A.; Freeman T. B.; Saporta S.; Janssen W.; Patel N.; Cooper D. R.; Sanberg P. R. Adult bone marrow stromal cells differentiate into neural cells in vitro. *Exp Neurol* 164(2): 247–256; 2000.

Singh R. P.; Shiue K.; Schomberg D.; Zhou F. C. Cellular epigenetic modifications of neural stem cell differentiation. *Cell Transplant* 18(10): 1197–1211; 2009.

Sterneckert J.; Höing S.; Schöler H. R. Concise review: Oct4 and more: the reprogramming expressway. *Stem Cells* 30(1): 15–21; 2012.

Streckfuss-Bömeke K.; Vlasov A.; Hülsmann S.; Yin D.; Nayernia K.; Engel W.; Hasenfuss G.; Guan K. Generation of functional neurons and glia from multipotent adult mouse germ-line stem cells. *Stem Cell Res* 2(2): 139–154; 2009.

Sun T.; Wang X. J.; Xie S. S.; Zhang D. L.; Wang X. P.; Li B. Q.; Ma W.; Xin H. A comparison of proliferative capacity and passaging potential between neural stem and progenitor cells in adherent and neurosphere cultures. *Int J Dev Neurosci* 29(7): 723–731; 2011.

Sundberg M.; Andersson P. H.; Åkesson E.; Odeberg J.; Holmberg L.; Inzunza J.; Falci S.; Öhman J.; Suuronen R.; Skottman H.; Lehtimäki K.; Hovatta O.; Narkilahti S.; Sundström E. Markers of pluripotency and differentiation in human neural precursor cells derived from embryonic stem cells and CNS tissue. *Cell Transplant* 20(2): 177–191; 2011.

Suon S.; Jin H.; Donaldson A. E.; Caterson E. J.; Tuan R. S.; Deschennes G.; Marshall C.; Iacovitti L. Transient differentiation of adult human bone marrow cells into neuron-like cells in culture: development of morphological and biochemical traits is mediated by different molecular mechanisms. *Stem Cells Dev* 13(6): 625–635; 2004.

Techawattanawisal W.; Nakahama K.; Komaki M.; Abe M.; Takagi Y.; Morita I. Isolation of multipotent stem cells from adult rat periodontal ligament by neurosphere-forming culture system. *Biochem Biophys Res Commun* 357(4): 917–923; 2007.

Traganos F.; Darzynkiewicz Z.; Sharpless T.; Melamed M. R. Simultaneous staining of ribonucleic and deoxyribonucleic acids in unfixed cells using acridine orange in a flow cytofluorometric system. J Histochem Cytochem 25(1): 46–56; 1977.

Uwanogho D.; Rex M.; Cartwright E. J.; Pearl G.; Healy C.; Scotting P. J.; Sharpe P. T. Embryonic expression of the chicken Sox2, Sox3 and Sox11 genes suggests an interactive role in neuronal development. *Mech Dev* 49(1–2): 23–36; 1995.

Uzbekov R. E. Analysis of the cell cycle and a method employing synchronized cells for study of protein expression at various stages of the cell cycle. *Biochemistry (Mosc)* 69(5): 485–496; 2004.

Vadivelu R. K.; Yeap S. K.; Ali A. M.; Hamid M.; Alitheen N. B. Betulinic acid inhibits growth of cultured vascular smooth muscle cells in vitro by inducing g(1) arrest and apoptosis. *Evid Based Complement Alternat Med* 2012: 251362; 2012.

Valcz G.; Krenács T.; Sipos F.; Leiszter K.; Tóth K.; Balogh Z.; Csizmadia A.; Muzes G.; Molnár B.; Tulassay Z. The role of the bone marrow derived mesenchymal stem cells in colonic epithelial regeneration. *Pathol Oncol Res* 17(1): 11–16; 2011.

Wakamatsu Y.; Nakamura N.; Lee J. A.; Cole G. J.; Osumi N. Transitin, a nestin-like intermediate filament protein, mediates cortical localization and the lateral transport of Numb in mitotic avian neuroepithelial cells. *Development* 134(13): 2425–2433; 2007.

Warthemann R.; Eildermann K.; Debowski K.; Behr R. False-positive antibody signals for the pluripotency factor OCT4A (POU5F1) in testis-derived cells may lead to erroneous data and misinterpretations. *Mol Hum Reprod* 18(12): 605–612; 2012.

Wilson P. G.; Stice S. S. Development and differentiation of neural rosettes derived from human embryonic stem cells. *Stem Cell Rev* 2(1): 67–77; 2006.

Woodbury D.; Schwarz E. J.; Prockop D. J.; Black I. B. Adult rat and human bone marrow stromal cells differentiate into neurons. *J Neurosci Res* 61(4): 364–370; 2000.

Zheng Y. M.; Dang Y. H.; Qiu S.; Qi Y. P.; Xu Y. P.; Sai W. J. Differentiation and characteristics of the enhanced green fluorescent protein gene transgenic goat neural stem cells cultured in attached and non-attached plates. *Cell Biol Int* 35(8): 849–856; 2011.

Zuk P. A. The intracellular distribution of the ES cell totipotent markers OCT4 and Sox2 in adult stem cells differs dramatically according to commercial antibody used. *J Cell Biochem* 106(5): 867–877; 2009.